UNIVERSITÀ DEGLI STUDI DI PADOVA
Facoltà di Scienze MM.FF.NN.
Facoltà di Ingegneria

ISTITUTO NAZIONALE DI FISICA NUCLEARE
Laboratori Nazionali di Legnaro

MASTER Thesis in
"Surface Treatments for Industrial Applications"

A NEW DESINGN OF PLANAR MAGNETRON SPUTTERING FOR HIGH UNIFORMITY TARGET EROSION

Supervisor : Prof. Vincenzo Palmieri
Assistan supervisor : Dott. Giorgio Keppel

Student: Ing. Gonzalez, Winder A.
Matr. N°: 878922

Academic year 2008-2009

A new design of planar magnetron sputtering for high uniformity target erosion

Winder A. Gonzalez

December 17, 2009

Introduction

Vacuum coating processes use a vacuum environment and an atomic or molecular condensable vapor source to deposit thin films, typically less than 5μm in thickness. An example of such a process is magnetron sputtering where material is removed from a solid target by ion bombardment and deposited on a substrate in atomic layers. It is one of the most flexible and controllable methods of generating a metal vapour in vacuum. Applications include low friction coatings for tools, anti-reflective coatings on glass, semiconductors, decorative coatings e.g. bath taps, touch panel screens, car headlamps, telescope mirrors and coatings for photovoltaics.

A magnetron sputtering source is composed by a cathode, an anode and a combined electric and magnetic field. There are various types of magnetron depending on the application and the target efficiency required. Each type requires an optimized design of magnetic field to ensure operation of the magnetron source. As the price of raw materials becomes higher, the efficiency of the usage of the deposition materials also becomes an important concern.

The purpose of a magnetic field in a sputtering plasma is to increase the efficiency of ionization by capturing electrons emitted from the target to enlarge the rate of the collisions between electrons and neutral gas atoms. The lack of uniformity of the magnetic field produces a non-uniform plasma density, hence differential sputtering rates across the surface of the target. It is obvious that increasing uniformity of the magnetic field will improve the uniformity of the erosion of the target.

This thesis shows the setup of a d.c. magnetron sputtering configuration for a target of copper 4$''$, based on a computational study of different magnetic confinements [8], as well as with an optimization of the erosion sputtered from the target. After the establishment of a minimum potential of the magnetic field to create gaseous plasma, some changes were made to optimize the erosion

pattern on the target surface and identify the possible control parameters. This work proposes a method of control on the magnetic field distribution applied on a new configuration of magnetron sputtering to extend the plasma distribution on the cathode surface. In order to try optimize the target erosion.

In particular the magnetic field of magnetron sputtering source used, is generated by two concentric copper coils. The main idea is to change the current of the coil in order to modify the magnetic field path. With a particular magnetron we will try to obtain an improvement of the target erosion. The idea is, in fact, to move the plasma on the target surface. The parameter that influence this rastering of the surface and that must be studied and correlated are the current of the coils, and the waveform of this current.

Contents

List of Tables

List of Figures

Chapter 1

Physical vapor deposition

Physical Vapor Deposition, or (PVD), is a term used to describe a family of coating processes. The most common ones are evaporation and sputtering. All these processes occur in a vacuum molecular regime and generally involve a bombardment of the substrate to be coated with energetic positively charged ions during the coating process to promote thin films growing. The glow discharge theory, based on the studies of electrical conductivity of gases considers the basic aspects about of sputtering. Additionally, reactive gases such as nitrogen, acetylene or oxygen may be introduced into the vacuum chamber during the deposition process in order to create various compound coating depositions. Some applications areas are aerospace and defense, architectural, glass, automotive, data storage, decorative, electronics, microelectronics, energy, lighting, medical, optics, security, wear coatings [12]. Fig.(1.1).

Figure 1.1: *Example of some PVD Applications areas*

1.1 Magnetron sputtering

One of the most common used PDV techniques is magnetron sputtering. This is a process used to deposit thin films of a material onto a surface or substrate and can be described as a creation of the gaseous plasma, where the source material called *target* is eroded by the ions arriving via energy transfer and is ejected in the form of neutral particles, either individual atoms, clusters of atoms or molecules.

As these neutral particles are ejected they will travel in a straight line unless they come into contact with some other particles or a surface nearby. If a *substrate* is placed in the path of these ejected particles it will be coated by a thin film of the source material.

1.1.1 Sputtering techniques

Sometimes the plasma is described as the fourth state of matter *gaseous plasma*, which is actually a dynamic condition where we can find neutral gas atoms, ions, electrons and photons existing in a near balanced state simultaneously. An energy source is required to *feed* and to maintain the plasma state while the plasma is losing energy into its surroundings. One can create this dynamic condition by introducing a gas (e.g. Ar) into a pre-pumped vacuum chamber and allowing the chamber pressure to reach a specific level and introducing a difference of potential between two electrodes into this low pressure gas environment, the pressure is in the range of $10_{-3} - 1\ mbar$ and the difference of the potential is around of $1000\ V$.

using a vacuum feed through.

There are two methods of sputtering: *(a)* Plasma sputtering and *(b)* ion beam sputtering. Plasma sputtering can be described as a triode system, in which the discharge is fed and maintained by the electrons of the thermionic cathode and not by γ electrons from the glow discharge cold cathode. The advantage of this is that sputtering can be maintained without a magnetic field even at lower gas pressure (low *mbar* region) than in a d.c. glow discharge where $p > 3 \cdot 10^{-2}\ mbar$. Applying a negative voltage with respect to plasma or anode, results in creating a positive-ion sheath, through which the ions stream from the plasma towards the electrode. The sheath thickness d is given by

Langmuirs space-charge equation (1.1).

$$J^{+} = \frac{U^{\frac{3}{2}}}{d^{2}} \tag{1.1}$$

Where J^{+} is ion current density at the sheath edge, d is the sheath thickness and U the difference voltage between target and plasma. Plasma electrons in the electrode vicinity are repelled so there is no excitation of gas atoms; the sheath is dark and clearly visible. Increasing the applied voltage will result in pushing the sheath edge farther away from the electrode. Ion-sheath thickness is independent of gas pressure as long as the ion current density remains constant.

1.1.2 The self sustained glow discharge

If a d.c. voltage is applied between two electrodes spaced at some distance d apart in a gas at low pressure $(10^{-2} - 1)$ *mbar*, a small current will flow [13]. This is caused by a small number of ions and electrons, which are always present in a gas due to ionization, by cosmic radiation. On their way from the cathode to the anode, the electrons make a fixed number of ionizing collisions per unit length. Each ionization process produces further electrons, while the resulting ions are accelerated toward the cathode. If the applied voltage is high enough, ions striking the cathode can eject secondary electrons from its surface. Emission ratio of secondary electrons of most material is of the order of 0.1, so several ions needs to bombard a given area of the cathode to release another secondary electron. If the supplied power is not high enough, the bombardment is concentrated near the edges of the cathode. When the power supplied increases, the bombardment entire covers the cathode surface and a constant current is achieved. The two processes of ionization by electron impact and secondary emission of electrons by ions, control the current I in the system, described by equation (1.2)

$$I = \frac{Io \cdot exp(\alpha \cdot d)}{\gamma \cdot [exp(\alpha \cdot d) - 1]} \tag{1.2}$$

where Io is the primary electron current generated at the cathode by the external source; α is the number of ions per unit of length produced by the electrons; d is the spacing between the electrodes and γ is the number of secondary electrons emitted per incident ion.

According to *Townsend criteria*, $\gamma \cdot [exp(\alpha \cdot d) - 1] = 1$ if the voltage between the electrodes is raised, the current becomes infinite, see equation (1.2). In this case a gas break-down occurr; glow discharge self-sustained, as the number of secondary electrons produced at the cathode is sufficient to maintain the discharge. Breakdown voltage is a function of the product of pressure p and electrode distance d *(Paschen's law)*. Distribution of potential, field, space charge and current density in a glow discharge are visually seen as regions of varied luminosity. From a cross sectional view of a glow discharge we see primary interest the region marked as *Crookes Dark Space*, cathode Dark Space (see Figure (1.2)), In this region, the positive ions have accumulated and have formed the space charge.

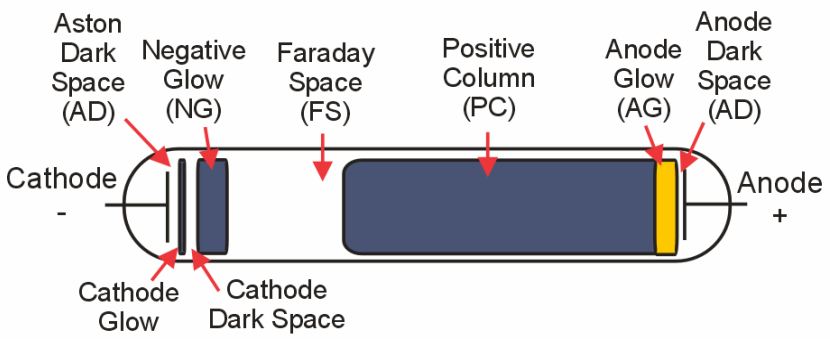

Figure 1.2: *Cross-sectional view of glow discharge.*

This thickness is approximately the mean distance traveled by an electron from the cathode before it makes an ionizing collision. The electron energies are over the maximum excitation potential which is insufficient to ionize gas molecules, so that no visible light is emitted. Electrons that leave the cathode with energy of the order of 1 eV are accelerated to sufficient ionizing energies in a region called *Aston's dark space*. The luminous region near to the cathode is *the cathode glow* where the electrons reach energies corresponding to the ionization potential. When the electrons reach the edge of the *negative glow*, they begin to produce significant numbers of ion-electron pairs. The number of slow electrons (i.e.those produced by an ionizing collision) has become very

large. The energy they possess is enough to cause only excitation and can't produce new ionization. Excitations caused by slow electrons are the reason of the appearance of the *negative glow*. In Faraday dark space the electron has insufficient energy to cause either ionization or excitation, consequently it is a dark space. *Faraday dark space* and the positive column are nearly field-free region with nearly equivalent number of ions and electrons. For glow discharge applied as sputtering sources, the positive column and the Faraday dark space usually do not exist, as the electrode separation needs to be small and the anode is located in the negative glow.

The exact mechanism by which atoms are ejected from a surface under ion bombardment are not known, but we can describe some of the details of the interactions involved. The figure (1.3) shows a brief description of the sputtering process.

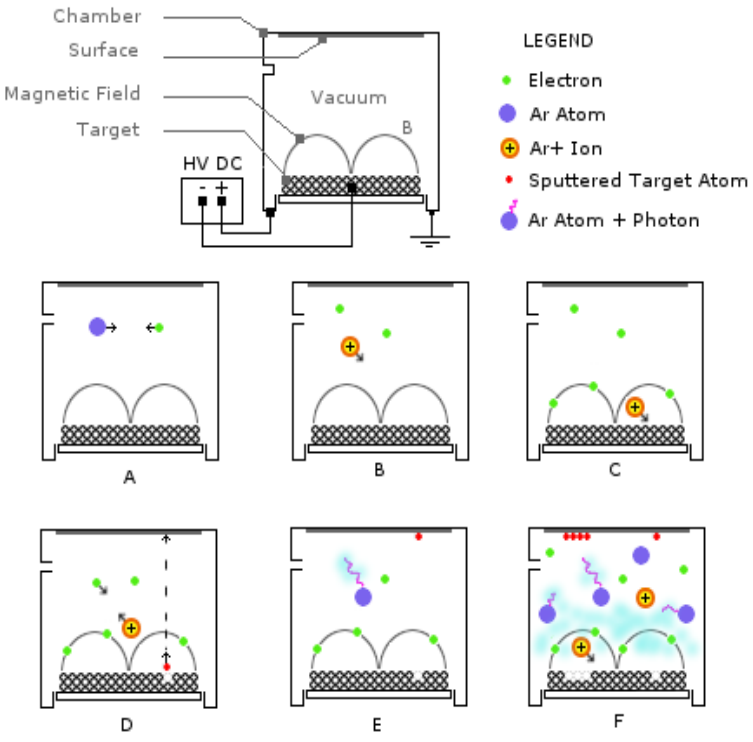

Figure 1.3: *Scheme of the sputter magnetron phenomenon: Ionization (A-B-C), Bombardment (C-D-E), Plasma (E-F).*

Ionization

Ever present *free electrons* will immediately be accelerated away from the negatively charged electrode *cathode*. These accelerated electrons will approach the outer shell electrons of neutral gas atoms in their path and, being a charge; will drive these electrons of the gas atoms [6]. This leaves the gas atoms electrically unbalanced since it will have more positively charged protons than negatively charged electrons thus it is no longer a neutral atom but a positively charged *ion* (e.g. Ar +). Figure.(1.3,A-B-C).

Bombardment

At this point the positively charged ions are accelerated into the negatively charged electrode *"cathode"* striking the surface and *blasting* loose electrode material (diode sputtering) and more free electrons by energy transfer. The additional free electrons feed the formation of ions and the continuation of the plasma. Figure.(1.3,C-D-E).

Plasma

All the while free electrons find their way back into the outer electron shells of the ions thereby changing them back into neutral gas atoms. Due to the laws of conservation of energy, when these electrons return to a ground state, the resultant neutral gas gained energy and must release that same energy in the form of photons. The release of these photons is the reason why the plasma appears to be glowing. Figure.(1.3,E-F).

1.1.3 Plasma confinement by magnetic fields

Within the sputtering process gas ions are accelerated out of a plasma towards a target consisting of the material to be deposited. The material is *sputtered* from the target and afterwards deposited on a substrate in the vicinity. The process is realized in a closed recipient, pumped down to a vacuum base pressure before deposition starts.

To enable the ignition of a plasma usually argon is supplied into the chamber up to a pressure

between 0.5 and $5 \cdot 10^{-3}$ *mbar*. By natural cosmic radiation there are always some ionized Ar+ ions available. In the dc-sputtering a negative potential V up to some hundred Volts is applied to the target. As a result, the Ar-ions are accelerated towards the target and set material free. On the other hand, they produce secondary electrons. These electrons cause a further ionization of the gas. The gas pressure p and the electrode distance d determine a break-through voltage from which on a self sustaining glow discharge starts following the equation (1.3), with materials constants A and B.

$$V_d = \frac{A \cdot p \cdot d}{ln(p \cdot d) + B} \tag{1.3}$$

The ionization rises with an increase in pressure and hence the number of ions and the conductivity of the gas also increase. The break through voltage drops. For a sufficient ionization rate a stable burning plasma results, where from a sufficient amount of ions is available for sputtering of the material.

To increase the ionization rate by emitted secondary electrons even further, a source of magnetic field is used below the target in the magnetron sputtering. The electrons are trapped in its field and *confined* in cycloids and circulate over the targets surface. This causes a higher ionization due to the longer dwell time in the gas and hence forms a plasma ignition at pressures, which can be up to one hundred times smaller than for conventional sputtering (diode sputtering).

Higher deposition rates can be realized thereby. On the other hand less collisions occur for the sputtered material on the way to the substrate because of the lower pressure and hence the kinetic energy at the impact on the substrate is higher. The electron density and hence the number of generated ions is highest where the $\vec{B}$ component of the magnetic field is parallel to the substrate surface. The highest sputter yield happens on the target area right below this region.

The bombardment of a non-conducting target with positive ions would lead to a charging of the surface and subsequently to a shielding of the electrical field. The ion current would die off. Therefore, the dc-sputtering is restricted to conducting materials like metals or doped semiconductors.

1.2 Sputtering configurations

Sputtering is a technique by which atoms and ions of argon or other gases coming from a plasma bombard a target by knocking atoms off of it. These material atoms travel to substrate where they are deposited and form a thin film. The simple configuration of a sputtering source is shown in figure (1.3). Diode sputtering consists of two electrodes placed in a vacuum chamber.

An anomalous glow discharge between 2 electrodes is created if a d.c. voltage of 500 V is applied. The substrate where the film is deposited is placed on the anode, while the target that will be sputtered represents the cathode (The negative electrode). High or ultrahigh vacuum is necessary to achieve thin film purity. After evacuation to high vacuum or ultra high vacuum (UHV), the chamber is filled with the sputtering gas, usually Argon, at a pressure of $(10^{-3} - 10^{-1})$ $mbar$. Applying a d.c. voltage of 500 V between cathodes will create a glow discharge that will ionize the argon gas. Positive ions of argon will be accelerated towards the cathode and due to their high kinetic energy particles will eject from the target surface. The ejected atoms have energies of the range of several eV. They will diffuse in chamber, following the cos^{-1} law till they condense on the surface of the substrate. The high kinetic energy of the sputtered atoms leads to a better adhesion and higher density of the sputtered thin film. The number of ejected atoms per incident ion is called sputtering yield.

The minimum ion energy required to dislodge target atoms is called sputtering threshold. The sputtering yield increases exponentially above the sputtering threshold $(10 - 30\ eV)$, then linearly, then less linearly till it approaches a flat maximum at energies of 10 keV . Further increasing the ion energy, the ion implantation effect takes place and the sputtering yield decreases. The sputtering yield and the resulting film properties can be controlled by adjusting the following sputter parameters:

The atomic number of the collision atoms

The influence of the masses of the target atom on energy transfer can be described as (1.4), where m = mass of target atom and M = mass of ion. That means that for a high sputtering yield the mass of the target atom should be not very different from the mass of bombarding ion.

$$E = \frac{4 \cdot m \cdot M}{(m+M) \cdot 2} \tag{1.4}$$

Sputter current

The sputtering current of the magnetron mainly determines the deposition rate of process. This parameter is directly related to the thin film grown process, in particular it can influence the coating quality introducing stress into the film.

Magnetron voltage

The applied voltage determines the maximum energy; with which sputtered particles can escape from the target (reduced by the binding energy). The applied voltage determines also the sputter yield, which is the number of sputtered particles per incoming ion.

The pressure

The pressure in the sputter chamber determines the mean free path or the sputtered material, which is proportional to $\frac{1}{p}$, together with the target substrate distance the pressure controls.

1.2.1 Magnetron configurations

For an effective sputtering, primary electrons must be used effectively to make sufficient ionization collisions in the vicinity of the cathode [7]. The efficiency of the available electrons can be increased if the plasma is confined by a magnetic field parallel to the cathode surface. A general rule for shape of the magnetic field is: *Magnetic field lines must be born from the cathode and die onto the target*. A plasma confinement is achieved, while magnetic or electrostatic mirrors trap the electrons [9]. Magnetic field traps and forces electrons to describe helical paths around the lines of magnetic forces. (see Figure 1.4)

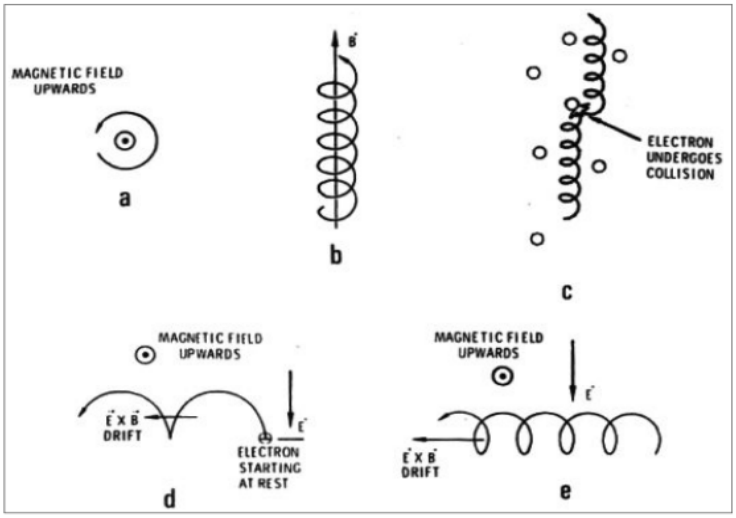

Figure 1.4: *Electron motions in static magnetic and electric field;* ***Legend:*** *a.-Electron motion in a magnetic field seen from up to down; b.-Electron drift along the magnetic field lines; c.-Movement of the electron when undergoing a collision; d.-Movement of the electron in a electro-magnetic field when there is an electric field component* $\vec{E}\perp\ (Volts/cm)$ *perpendicular to* $\vec{B}$*; e.- Electron has a drift speed* $\vec{E}\times\vec{B}$ *in a electromagnetic field.*

When $\vec{B}$ is parallel to $\vec{E}$ the particles are freely accelerated, while when there is an electric field component $E\perp\ (Volts/cm)$ perpendicular to $\vec{B}$, a drift of speed V_E occurs.

$$V_E = 10^8 \cdot \left(\frac{E\perp}{B}\right)(cm/s) = 10^8 \cdot \left(\frac{\vec{E}\times\vec{B}}{B^2}\right) \tag{1.5}$$

When $\vec{B}$ is uniform and $\vec{E}$ is zero, the electrons drift along the magnetic field lines orbiting them with a cyclotron frequency ω_c and at the gyro or Larmor radius rg.

$$\omega_c = \left(\frac{eB}{m_e}\right) = 1,76 \cdot 10^7 \cdot B(rad/sec) \tag{1.6}$$

$$rg = \left(\frac{V_E}{\omega_c}\right) = \left(\frac{m_e}{e}\right)\left(\frac{V_E}{B}\right) = 3,37 \cdot \left(\frac{\sqrt{W\perp}}{B}\right)(cm) \tag{1.7}$$

Where $\vec{B}$ is in Gauss and $W\perp$ is the energy associated with the electron motion perpendicular to the field in eV.

The path that electron must travel is increased, thus increasing the probability of collision. The same effect can be achieved increasing the gas pressure. Using a magnetic field makes possible sputtering at lower pressure (10^{-3} $mbar$) or if the pressure is not reduced, to obtain greater sputtering current for a given applied voltage. This on the other hand causes strong target heating making necessary a target cooling system. As the electrons can move freely along the field lines, end losses are possible. The problem is eliminated installing reflecting surface wings (mirrors) maintained at the cathode potential or by causing the magnetic field lines intersect the cathode. In order to complete the electrical circuit, the low energy electrons must be removed from the trap and migrate to the anode. It is believed that plasma oscillations assist in this process. Anode placement, size and design have an important role and it should take into account the poor mobility of the low-energy electrons. Proper anode placement and design can greatly reduce spurious electrical activity.

1.2.2 Target erosion

The uniformity of the target erosion determines the life of the target as well as the uniformity of the thin film created from it [13]. This reason motivates the study of the sputtered flux distribution (erosion shape) on the target. However, really few information is found in literature because the cost of the experiments required to measure the target erosion shape for different sputtering conditions is very high. In this sense, the erosion pattern of a magnetron sputter target has been investigated numerically [11],[13],[5] this is the basis of the this work.

1.2.3 The studied magnetron source

This work studies the influence of variations of magnetic field on the target erosion shape, in order to improve a method to control the erosion shape of the target during magnetron sputtering process. For this purposes,it has been generated a magnetic confinement by two coils instead of permanent magnets that are usually used.

The current variations applied to the coils, external current I_{ext} and Internal current I_{int} can produce a variation of the magnetic field over the target surface. Figure (1.6), Consequently the plasma confined by this magnetic field can be moved along the target surface, As a result of this control some regions of the target can be erode preferentially, inducing a uniform consumption of the target material [11].

1.2.4 Considerations for magnetron design

In general, a magnetron sputtering source is a device that satisfies the following *Penning condition* [11].

- An annular-like volume of space is threaded by lines of magnetic field which, at either end, intersect surfaces at cathode potential.
- A glow discharge is sustained by the application of a negative voltage to the cathode surface. The dominant voltage drop occurs across positive ion sheaths which form to the cathode surface.
- A magnetic field strength is high enough to *trap-γ electrons* released from the cathode surfaces by ion bombardment, until a substantial fraction of their energy is lost ionizing collisions with ambient gas molecules.
- A geometry is designed in a way to allow a substantial fraction of the gaseous ions produced in the trap volume to be attracted to, and collected by , the cathode surfaces which delimit such *trap-volume*. These ions are accelerated through the positive ion sheath to the cathode and cause sputter erosion of cathode material.

In particular a magnetron sputtering source must satisfy the following practical conditions:

- The sputter target will be the cathode that works as an electrostatic mirror for trapped electrons.

- The magnetic field lines must be *born* from the cathode and must *die* onto the target in order to enforce the magnetic confinement and not lose alectrons.

- The $\vec{E} \times \vec{B}$ induced drift current, following parallel to the cathode surface located adjacent to the cathode ion sheath, must run along closed paths, the sputter erosion track being determined by this self-closing flow of electrons.

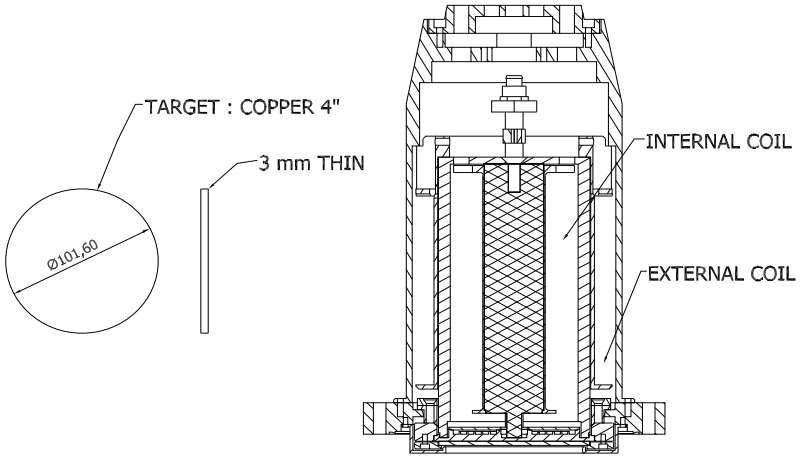

Figure 1.5: *Details: Target dimensions and magnetron coils.*

Using the desing rules explained above,it is possible to optimize the planar magnetron source. [10]. Starting from a circular planar magnetron in which the magnetic field is generated by a solenoid and adding another coil concentric to the first one and separated by an iron yoke, it is possible to vary the magnetic confinement changing the ratio between the currents flowing in the two coils, $\frac{I_{ext}}{I_{int}}$ Figure (1.5). Consequently,it is possible to confine the plasma over differents regions of target surface and erode preferentially some zone respect to others, achieving better material consumption.

Modulating the ratio $\frac{I_{ext}}{I_{int}}$ during the thin film deposition, the erosion path diameter can be controlled; Figure (1.6), shows three limiting cases of the ratio: $\frac{I_{ext}}{I_{int}}$ on the left image $I_{ext} \ll I_{int}$ and so plasma is confined on the external region of the target; on the central one, the current flowing through the external coil is nearly equal to the current flowing in the internal one and the plasma is

confined in an annular region around the center of the target, like in a standard magnetron source; in the right image $I_{ext} \gg I_{int}$ so the plasma is more dense over the target center.

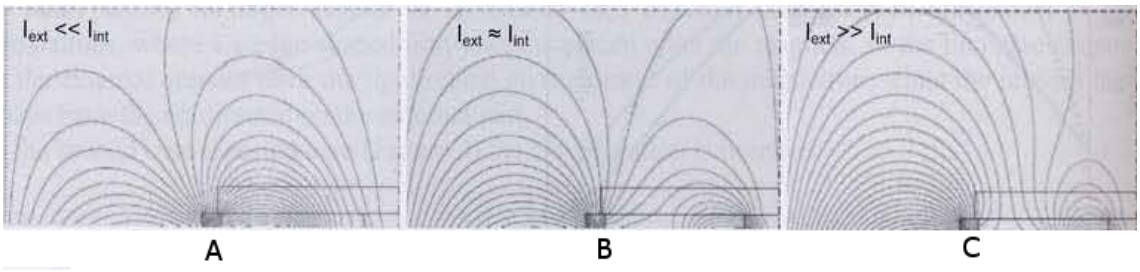

Figure 1.6: *Calculated magnetic field lines close to the target for the 4" magnetron source:(A)* $I_{ext} \ll I_{int}$*, (B)* $I_{ext} \approx I_{int}$*, (C)* $I_{ext} \gg I_{int}$*.[11].*

At fixed sputtering power we can raster the target surface by forcing the ratio $\frac{I_{ext}}{I_{int}}$ to oscillate at low frequency. With this configuration the oscillating frequency may be regulated to obtain an extremely uniform target erosion. This thesis is based on the control and test of the different combinations of the currents in order to obtain the control over the plasma confinement.

Chapter 2

Experimental setup

An experimental system has been assembled to study the target erosion and to look for the best parameter of I_{ext}, I_{int}, on waveform in order to obtain a uniform erosion of the target surface, the system is shows in the Figure (2.1). In this part there is a detailed description of the system used to control and test the different combinations of the currents for the driving of the magnetic field of 4" magnetron sputtering. The current of the target is fixed to 1 Amp, for all experiments reported in this thesis. Is very important not only choosing the most adequate work plan method, but also having a proper control on the parameters provided, and obtain the complete data from the acquisition system for an accurate experimental process.

2.1 General description

The experimental system basically consists in a vacuum chamber with a 4" magnetron source, a pumping system, three DC power supplies and a computer used to control the system and for the data acquisition. Figure (2.2) shows a scheme of it. The vacuum chamber is a cylindrical stainless-steel vacuum vessel of 50 cm diameter, and 50 cm height, with two viton seals on top and bottom,on two perpendicular tubes to the chamber there are two CF 150 flanges, on one there is installed the magnetron source, and on the other one there is the view port flange. Figure (2.3). This configuration permits the direct observation of the magnetron plasma because the flanges are on axis. The gas

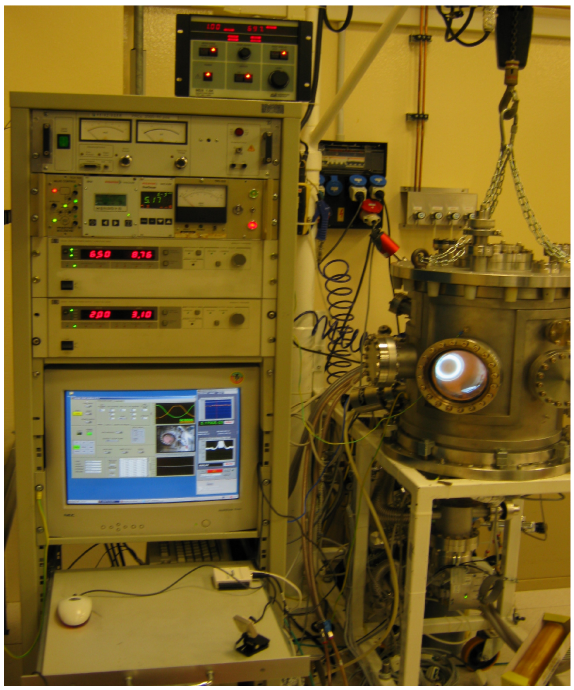

Figure 2.1: *Picture of the system: On the left: The PC for control and data acquisition, power supplies and the electronic control of the vacuum system. On the right: The vacuum chamber.*

employed is Ar and a manual leak valve regulates the flow. The vacuum chamber is evacuated by a turbomolecular pump connected to a primary rotary pump. During this work of thesis a software written in LabView^{TM}, with this software it is possible to control and measure some parameters of the system.

2.1.1 Magnetron description

The 4 ” magnetron sputtering source used is briefly described in figure (2.3). A hard plastic ring provides the electric insulation with the sputtering target being the only element facing the ultra-high vacuum (UHV) side. A viton O-ring is used for vacuum sealing. A thin layer of an indiumgallium alloy provides the thermal contact of the sputtering target to the copper base plate. The copper base plate is braised to the stainless-steel source body at about 800° C under vacuum by means of a Pd-Ag-Ni alloy. The copper base plate is water cooled and it thermally separates the target from the magnetron magnetic core, coaxial to the target. The cooling water flux of about 30 $l\ min^{-1}$

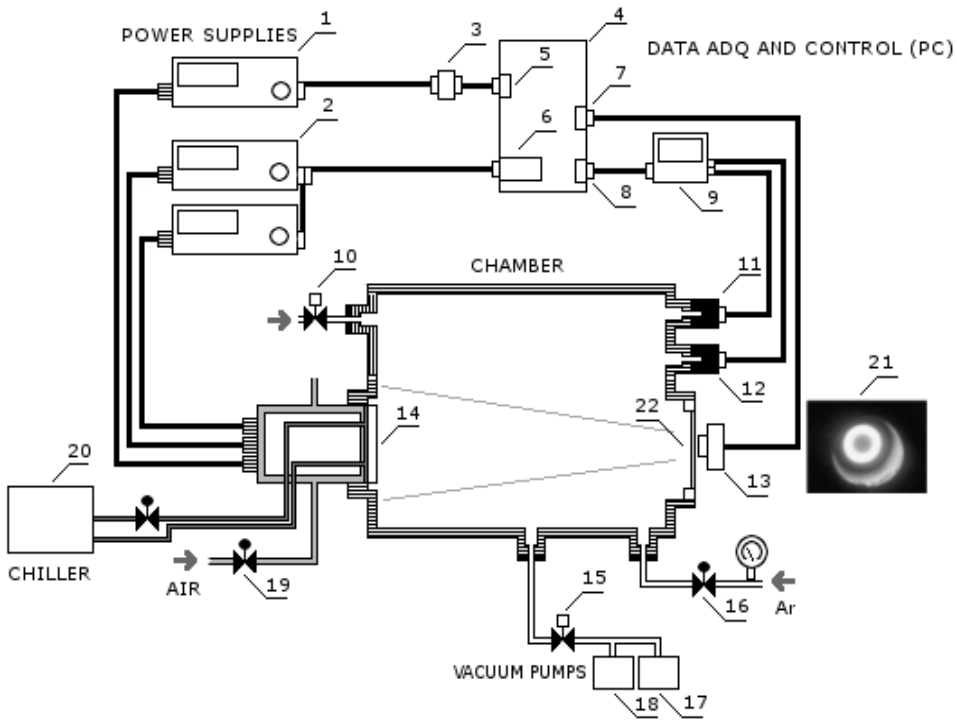

Figure 2.2: *Experimental system setup. In this figure we can see the scheme of all elements that compound the experimental system.* ***Legend:*** *1.-MDX 1,5 kW Magnetron power supply* ($720V/2A/1.5kW$) *Power Supply. 2.-HP 6032A System Power Supply* ($0-60V/0-50A/1000W$). *3.- NI USB 6009, 8 Inputs, 14-bit Multifunction I/O. 4.- PC. LabVIEW™ ver.8. 5.- USB Port. 6.- Card PCI Controller GPIB NI. 7.- USB Port. 8.- RS-232 Serial Port DB9. 9.- Dual Gauge™ Controller TPG 262. 10.- Valve VAT™* ($220-230V/50Hz/2W$). *11.- Pfeiffre Vacuum Compact Fullrange™ BA Gauge. 12.- Pfeiffre Vacuum D-35614 Asslar, TyP CMR 364. 13.- WebCam Generic 800x600 Pixels, RGB 24. 14.- Target (Copper, 4" Diameter). 15.- Gate Valve VAT™. 16.- Manual Valve Balzers. 17.- Turbomolecular Pump. 18.- Rotary Pump. 19.- Manual Valve (Air). 20.- Chiller Unit. 21.- Image obtained. 22.- View Port CF flange.*

at a pressure of 3 bar can sustain a discharge power of about 10 kW. Further cooling of the magnetic core is provided by a compressed air flow. In magnetron operation the plasma confinement is provided by two concentric coils surrounding a soft-iron yoke into which the magnetic circuit is closed. By switching on or off the current to the coils, the source can be operated both as a diode and as a magnetron.

In order to have an effective confinement, the magnetic field lines must originate from the target and must end in the target. Calling I_{ext} and I_{int} the currents circulating in the external and the internal coils, respectively, by changing their ratio the source can be operated both as a type 1 and type 2 unbalanced magnetron, according to the definition given by Window and Savvides [14] and Window and Harding [16]. The different magnetic configurations obtained by varying the ratio $\frac{I_{ext}}{I_{int}}$ were computed using the MAFIA code [10].

If the condition $I_{ext} \ll I_{int}$, holds, figure (1.6,a), not all of the magnetic field lines generated from the internal coil end up in the target. The electron trajectories are deflected tangentially to the target surface so that the interaction between the plasma and the substrate is minimal. Such a circumstance is very useful whenever sputtering occurs from complex targets, where it is important to suppress plasma resputtering and thermal desorption of high-vapour-pressure elements from the growing film. On the contrary, if $I_{ext} \gg I_{int}$, figure (1.6,b), the plasma is confined towards the target center. The electrons escaping by the primary toroidal trap are confined into a coaxial plasma torch perpendicular to the target. Such an unbalance of the discharge provides a kind of *plasma washing* of the growing films, which is of particular importance when sputtering high-purity transition metals, whose superconducting properties are crucially dependent on the amount of trapped impurities [11].

2.1.2 Control and data acquisition

Choosing good method to determine the best combination magnetron currents setup, means to understand which are the most sensible parameters involved in the process. Sometimes implementing automated tests can create as many problems as it solves. In this senses is necessary to apply the basic classification of the signals when is possible to make automating testing [17].

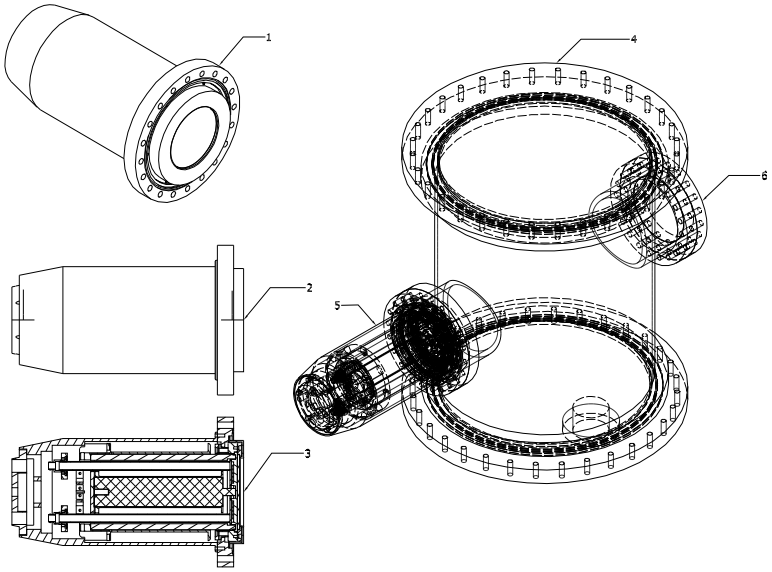

Figure 2.3: *General Description.* ***Legend:*** *1.-Magnetron, 2.-Target, 3.-Magnetron (Transversal section), 4.-Vacuum Chamber, 5.-View Port Flange*

Signals definition

Producing a block experimental requires to make the classification of the available signals to control and measure. For this reason it is necessary to identify which are the system facilities. In the following list we can see a classification of the parameters selected.

1. **Pressure chamber** (*measure*): Dual Gauge^{TM} Controller TPG 262, This driver provides the measure of two vacuum sensors, (capacitive and fullrange) via Serial RS-232 communication.

2. **Magnetron power supply** (*measure*): MDX 1,5 kW Magnetron Driver ($720V/2A/1.5kW$) Power Supply. The analog interface provides a proportional reference of current, voltage and power, in a scale of (0-5) $Volts$.

3. **Magnetron currents coils** (*measure and control*): (Two Units) Each system power supply is an autoranging GP-IB power supply and consequently can be used for remote control.

4. **Video, display plasma** (*acquisition*): WebCam Generic 800x600 Pixels, RGB 24. To acquire video via USB connexion.

5. **Time** (*measure*): PC, Counters in *msec* provides a reference time base (t_b).

Based on the control theory , the experimental setup is a typical *Open loop system* and can be described as in Figure(2.4). Normally the variable process is the system parameter that needs to be controlled, in our case *the plasma confinement*, by forcing the ratio $\frac{I_{ext}}{I_{int}}$ to oscillate at low frequency.

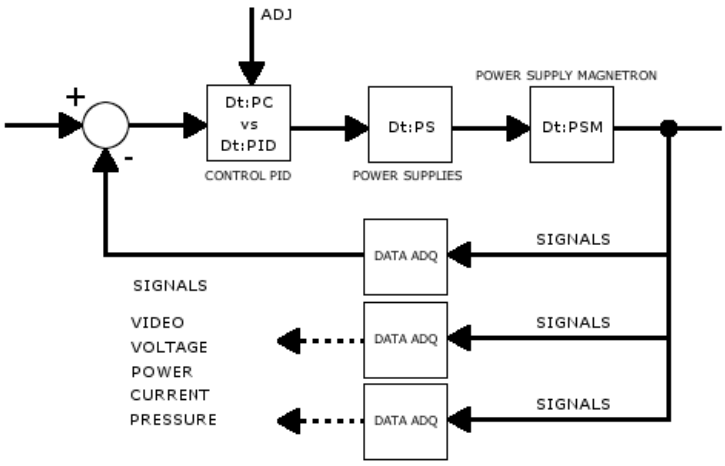

Figure 2.4: *The experimental setup: Block control*

To know the presence of the plasma on the target is easy through observation. However, to determine the exact position and confinement region is not easy. Therefore, this work proposes to take an indirect measurement that permits to identify a valid indicator of stability. For this reason it is necessary to make severals probes in order to determine which is the best and suitable control parameter. During the first probes of the video acquisition, it was determined that this is not a good way to control the experiment due to the fact a few minutes after the beginning of the sputtering process , the observation of the plasma is impossible because material is deposited on the view port. In constrast, the video acquisition was useful to analyze the plasma confinement on the target in the beginning of all the experiments. Figure (2.5).

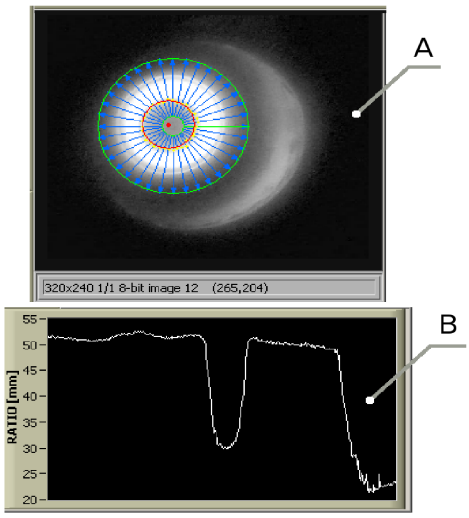

Figure 2.5: *Display plasma and ratio measurement. A) Video acquisition and best circle processing. B) Graphical results of the ratio measurement.*

2.1.3 GPIB Communication

The HP 6032A $(0-60V/0-50A/1000W)$, system power supply is an autoranging GP-IB power supply. It uses power MOSFETs in a 20 kHz switching converter to provide an autoranging output characteristic with laboratory performance. Output voltage and current are continuously indicated on individual displays. LED indicators show the complete operating state of the unit. Front-panel controls allow the user to set output voltage, current and overvoltage protection trip levels. Overvoltage protection (OVP) protects the load by quickly and automatically interrupting energy transfer if a preset trip voltage is exceeded. Foldback protection can be selected to disable the power supply output if the unit switches from Constant Voltage (CV) to Constant Current (CC) mode or vice-versa.

The power supply can be both a listener and a talker on the GP-IB, and can be programmed directly in volts and amps. Power supply status can be read over the GP-IB, and the power supply can be instructed to request service for any of ten conditions. Upon command, the power supply will measure its output voltage, output current, or OVP trip voltage and put the value on the GP-IB [15].

The following parameters and features are controlled by the developed software via the GP-IB:

- Output voltage setting (12 bits)
- Output current setting (12 bits)
- Output disable/enable
- Status reporting
- Foldback protection
- Output voltage measurement (12 bits)
- Output current measurement (12 bits)
- Machine state initialization
- Self test

2.1.4 R-232 Serial communication

Dual Gauge^{TM} Controller TPG 262, provides a serial interface, and this can be used for communication between the TPG 262 and a the computer. When the TPG 262 is in operation, it starts transmitting measured values in intervals of $1sec$. As soon as the first character is transferred to the TPG 262, the automatic transmission of measured values stops. After the necessary inquiries or parameter modifications have been made, the transmission of measured values can be started again by means of the commands [18].

2.2 Experimental parameters

Notice that the first experiments are based on the observation and search of the minimum levels of the currents combination of the coils that permit to maintain the switching on of the plasma. In this sense the experiments show that the minimum value of the currents combination are $(I_{ext} = 4, 1)A$

and $(I_{int} = 4,1)A$, in the same way the manual variation of the currents show the range of the current acceptable to confine the plasma over different regions of the target surface.

2.2.1 Magnetron currents

Through programing have been made two data vectors with 360 registers or *DAQ Data control and Acquisition* . Each vector contains an array of the values that describe the wave form $I(a,t)$, see equation (2.1) and (2.2), programmed by the user of the system. The time of the each program cycle is called time base t_b and this is a variable programmable, The t_b used for the experiments on: Target A, Target B and target C, is $t_b = 300msec$. In others words a program cycle occurs in the lap of $1,8$ minutes, *Low frequency*.

$$I_{int}(a,t) = \begin{cases} A + B \cdot \sin(\omega \cdot t) & 0 \leq t < \pi \\ A + C \cdot \sin(\omega \cdot t) & \pi < t \leq 2\pi \end{cases} \tag{2.1}$$

$$I_{ext}(a,t) = \begin{cases} A + D \cdot \sin(\omega \cdot t + \phi) & 0 \leq t < \pi \\ A + E \cdot \sin(\omega \cdot t + \phi) & \pi < t \leq 2\pi \end{cases} \tag{2.2}$$

$$\omega = \frac{2\pi}{360(samples) \cdot t_b} \tag{2.3}$$

Where a is the amplitude in amperes, t time, ω the angular frequency, t_b time base, ϕ angle between I_{int} and I_{ext},A-B-C-D. wave parameters defined in figure (3.1). The first results showed in figure (2.6), were obtained with the wave form described in the table (3.1.2, Target A).

After establishing the initial experimental conditions, it is necessary to prevent the different sources of the fails such as the target cooling, leaks, short circuit on the magnetron, etc. For instance, in our case , our goal is to make a total erosion of the target, therefore, some portions of the material sputtered would be deposited on an isolated area, causing a short circuit. For this reason is very important to have a continuous control on the system. Some experiments weren't overcome successfully. However, three of them are reported through observation and experimentation, also supported on the data acquisition.

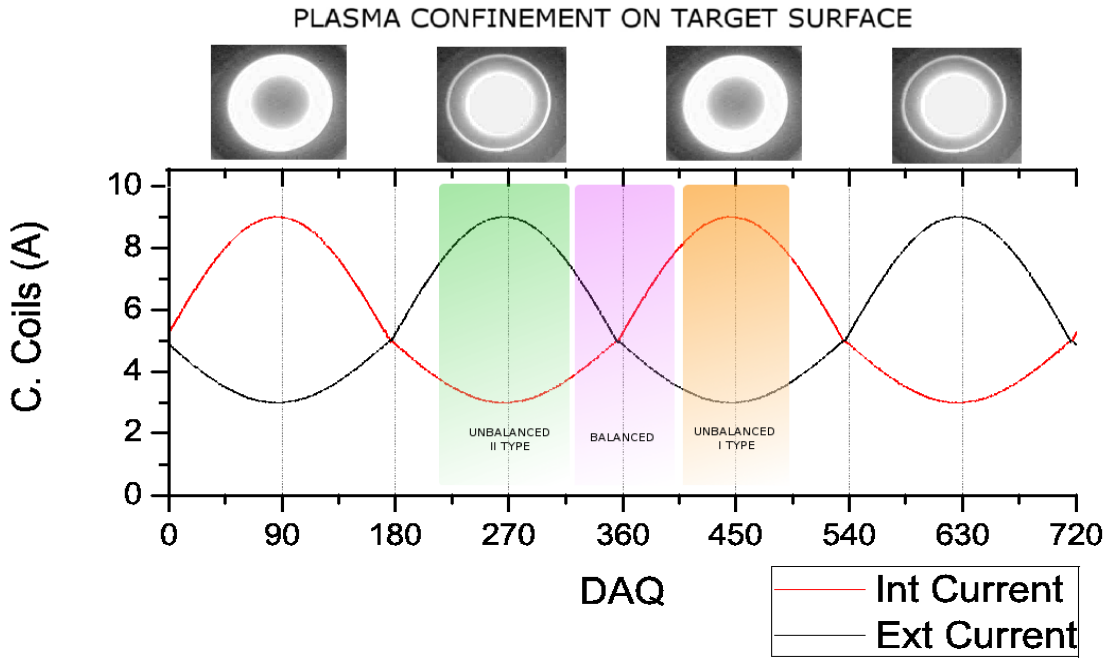

Figure 2.6: *Switching on the plasma and confinement, balance, unbalanced I/II type regions.*

2.2.2 Pressure

As mentioned before, the main chamber can be directly evacuated to a pressure in the low $(5 \cdot 10^{-5})$ *mbar* by a turbomolecular pump. In figure (2.7) we can see a typical profile of the pressure chamber during a test. Notice that the range selected is between $(8 \cdot 10^{-3} - 5 \cdot 10^{-3})$ *mbar* for all the experiments.

2.3 Experimental program

The experimental process require a detail plan of work , in this sense a flowchart was developed, this represents the general algorithm used during each test. In figure (2.8) we can see the steps as boxes of various kinds of sub-routines program, and their order by connecting these with arrows. The program control of the system was made in event-based programming in which the flow of the program is determined by events i.e., sensor outputs or user actions (controls or signals) or messages from other programs or threads.

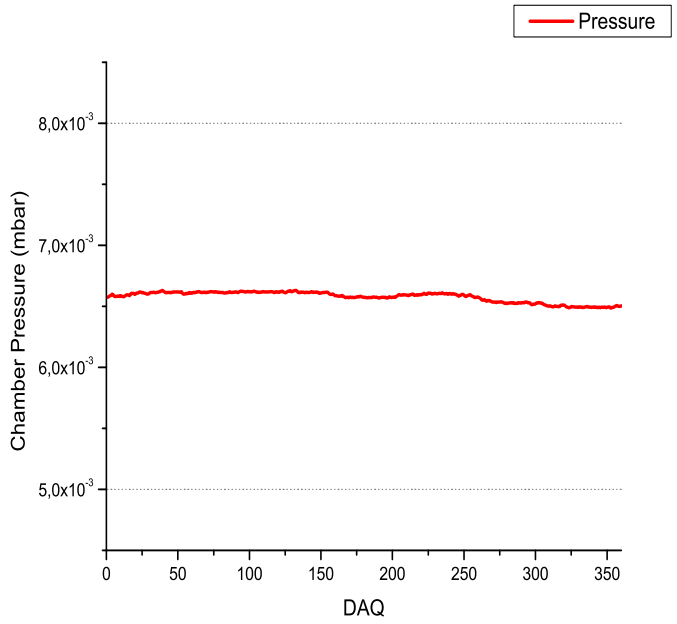

Figure 2.7: *Experimental profile pressure*

The time control over the magnetron currents is not a critical parameter, for this reason is possible to select a baud rate close to ($t \gg \frac{1(cycle)}{min}$) *low frequency*, As consequence of this the time process of the operating system it's not a problem. The baud rate selected was 300 *msec* for each cycle of the program, In figure (2.9), we can see an graphical representation of the program cycle rate. Notice that the non linear variation are introduced by the internal process of the operating system.

The program developed to control the system was built on LabVIEW^{TM}, it is defined as a graphical programming environment to develop measurement, test, and control systems using intuitive graphical icons and wires that resemble a flowchart. The program designed is called a virtual instruments (VIs). And this is composed of two principal parts.In figure (2.10), we can see a brief description of the front panel designed for the system control.

1. **Front Panel** How the user interacts with the VI.

2. **Block Diagram** The code that controls the program.

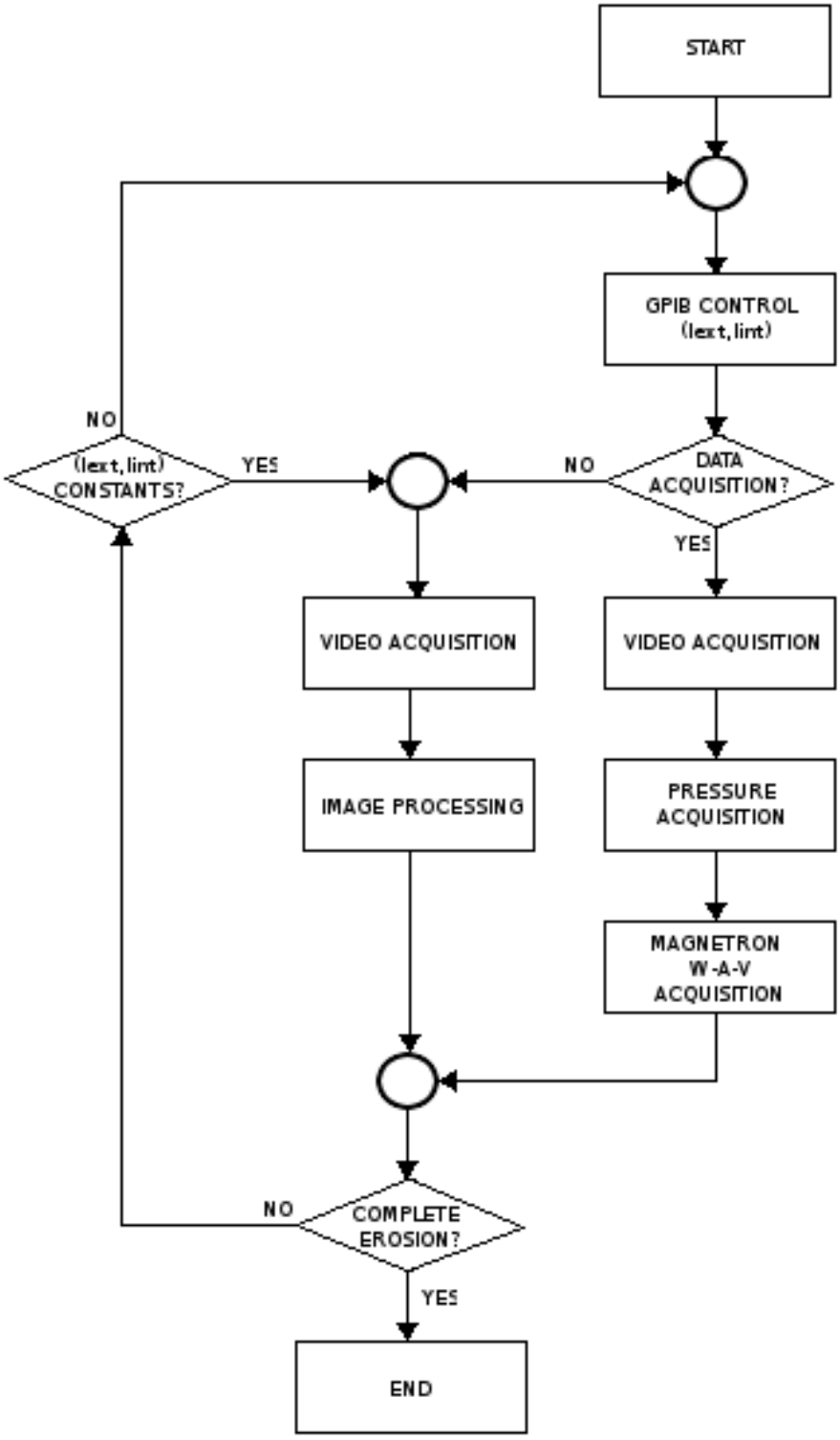

Figure 2.8: *Experimental flowchart of the program*

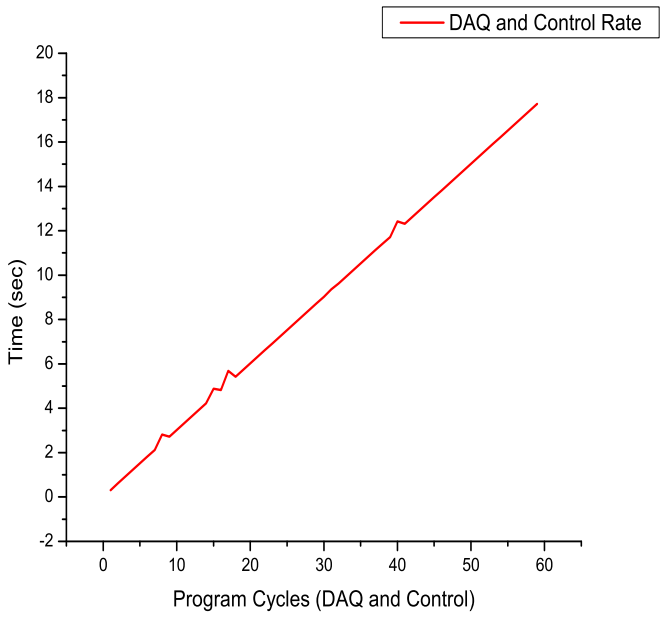

Figure 2.9: *Program cycle rate. Each DAQ (Data control and acquisition) represent a program cycle.*

2.3.1 Front panel of the program

The Front Panel is used to interact with the user when the program is running. Users can control the program, change inputs, and see the data updated in real time. Where the controls are used for inputs , turning a switch on or off, or stopping a program. Indicators are used as outputs. Graphics, lights, display video, and other indicate values from the program. These may include data, program states, and other information.

Every front panel control or indicator has a corresponding terminal on the block diagram. When a VI is run, values from controls flow through the block diagram, where they are used in the functions on the diagram, and the results are passed into other functions or indicators.

The front panel is the user interface of the VI. and this is building with controls and indicators, which are the interactive input and output terminals of the VI, respectively. Controls are knobs, pushbuttons, dials, and other input devices. Indicators are graphs, LEDs, and other displays. Controls simulate instrument input devices and supply data to the block diagram of the VI. Indicators

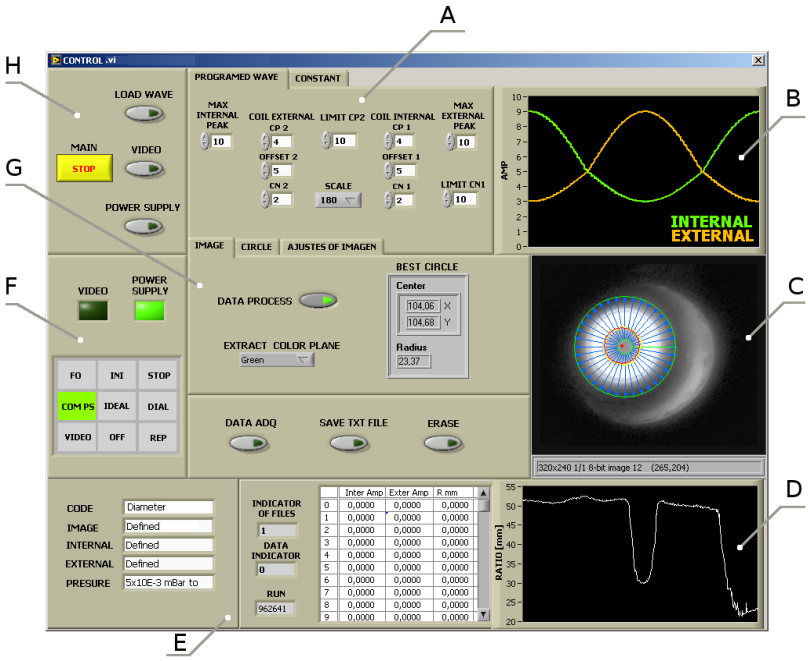

Figure 2.10: *Front panel of the program.* ***Legend:*** *A) Currents Wave setup; B) Display current-out; C) Display plasma and ratio measurement; D) Graph: Ratio measurement; E) Data setup; F) Program stage; G) Image setup analysis; H) Master control.*

simulate instrument output devices and display data the block diagram acquires or generates.The following list offers a brief description of the front panel.

- **A) Currents Wave setup**: Allows to modify the wave form supplied to the magnetron coils.
- **B) Display current-out**: This graph shows the values of the current out of each HP 6032A system power supply.
- **C) Display plasma**: This graph shows the video acquisition.
- **D) Graph: Ratio plasma measurement**: This graph shows the result of the video processing
- **E) Data setup**: This area allows to identify each experience by name and numeric code.
- **F) Program stage**: Shows the actual stage of the program.
- **G) Image setup analysis**: Permit to modify the criteria of the video processing.

- **H) Master control.**: Switches on or off, or stop a sub-routine of the program.

2.3.2 Block diagram of the program

The block diagram contains this graphical source code. Front panel objects appear as terminals on the block diagram. Additionally, the block diagram contains functions and structures from built-in LabVIEW™ VI libraries. Wires connect each of the nodes on the block diagram, including control and indicator terminals, functions, and structures.

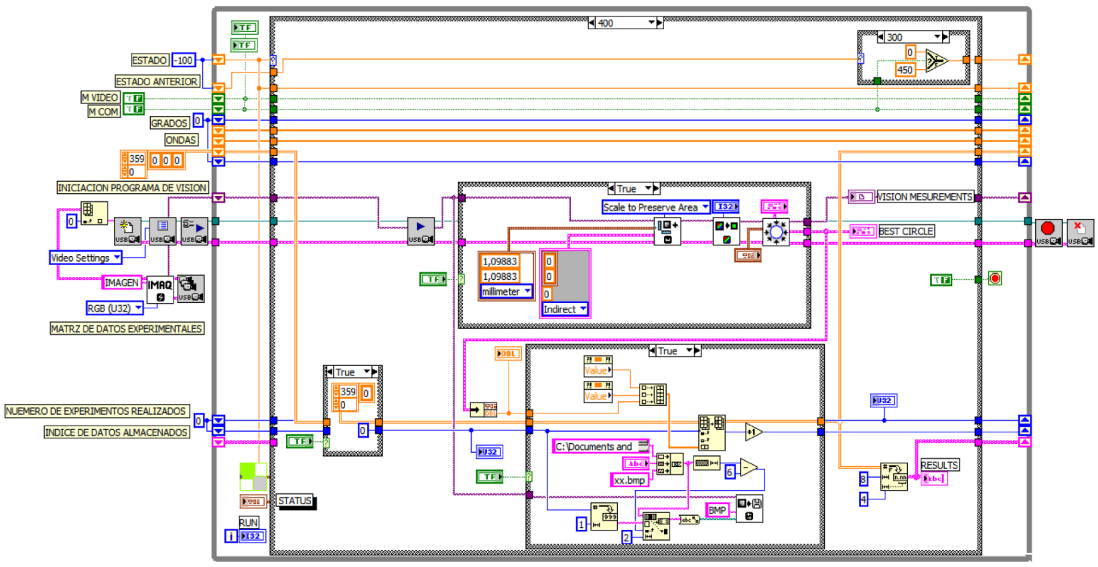

Figure 2.11: *Block diagram of the program*

2.3.3 Stage machine

The program was developed as a model of behavior composed of a finite number of states *finite state machine*, transitions between those states, and actions. Similar to a *flow graph* where we can inspect the way in which the logic runs when certain conditions *events* are met.

A current state is determined by past states of the system. As such, it can be said to record information about the past, i.e., it reflects the input changes from the starting of the system to the present moment. A transition indicates a state change and it is described by a condition that would

need to be on to enable the transition. An action is a description of an activity that is to be performed at a given moment. In figure (2.12), we can see a scheme used to build the program.

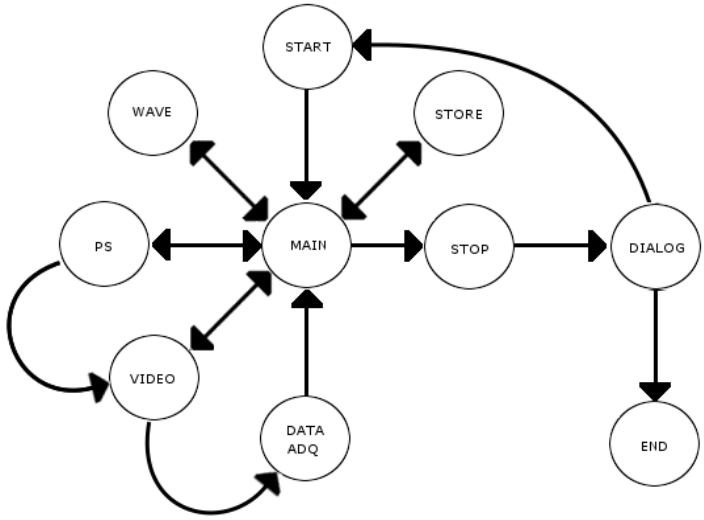

Figure 2.12: *Stage diagram:* ***Legend:*** *START (Initial stage). WAVE (Algorithm for calculating wave forms). PS (Algorithm for communication via GPIB). VIDEO (Algorithm for analysis and video acquisition). DATA ADQ (Algorithm for communication via serial R-232 and USB). STORE (Algorithm for safe data in TXT format). STOP (Safety exit). DIALOG (User Interface). MAIN (Algorithm based in events).*

Chapter 3

Results

This chapter shows the results obtained during the experimental process. The results are presented and discussed in function of the difficulties to overcome in the course of the investigation.

3.1 Experimental system

In order to understand how the variations of current affect the plasma confinement was created an experimental system to make several test on the 4" magnetron source, and to identify the available parameters to control the erosion path of the target (3.1). In addition was created an experimental work plan built on a model of an open-loop control system, where the system is controlled directly, and only, by an input signal, without the benefit of feedback.*Open loop system* which is the base of the program developed to control the system.

The first experiments was made in order to found the minimum levels of the currents combination that permit to maintain switched on the plasma. The currents combination are $(I_{ext} = 4,1)\,A$ and $(I_{int} = 4,1)\,A$. Furthermore, the results of sequential manual experiment show the range of the current acceptable to confine the plasma over different regions of the target surface, calculated by the equations (3.1) and (3.2).

$$I_{int}(a,t) = \begin{cases} A + B \cdot \sin(\omega \cdot t) & 0 \leq t < \pi \\ A + C \cdot \sin(\omega \cdot t) & \pi < t \leq 2\pi \end{cases} \tag{3.1}$$

Samples	Weight before (gr)	Weight after (gr)	Percent of material sputtered %
Target A	213,45	114,45	46,32
Target B	206,96	114,78	44,54
Target C	214,88	101,66	52,69

Table 3.1: *Initial weight and percent of material sputtered*

$$I_{ext}(a,t) = \begin{cases} A + D \cdot \sin(\omega \cdot t + \phi) & 0 \leq t < \pi \\ A + E \cdot \sin(\omega \cdot t + \phi) & \pi < t \leq 2\pi \end{cases} \tag{3.2}$$

The phase between each wave current ϕ represent the differential angle used to produce different kinds of the currents setup. In our case ϕ was fixed as 180° for all the experiments, because, this value of the ϕ to permit the maximum difference between I_{int} and I_{ext} Consequently,it is possible to confine the plasma over different regions of target surface and erode preferentially some zone respect to others. In addition exist other parameter defined as *scale*, Figure (3.1) and this one is used to produce the modification of the relative time between each half cycle.

During the experimental process some tests weren't overcome successfully because of a bad thermal contact between the target and the magnetron source. However three of them was completed successfully. Figure (3.2), *total erosion.* The results will be discussed in the next part.

3.1.1 Erosion pattern

Before the sputtering process each target was cleaned by ultrasound and weighted in other to compare, after the sputtering process, how much material was sputtered. Finally the cross section of the targets was digitalized and measured. In the following table we can see the results obtained for three different currents setup classified as Target A, Target B and Target C. Table (3.1.1).

3.1.2 Graphic results

The profile erosion obtained for each test Target A-B-C, can be observed by means of the digitalization of the cross section. Figure (3.4).

The direct observation of the plasma on the target surface and the erosion profile result, are the basic criteria to justify the modification of the current setup for each different test. In the following table (3.1.2), we can see the parameters of the current setup selected by each experiment.

Parameters	A	B	C	D	E	F	Scale
Target A	5	4	2	4	2	N/A	1:1
Target B	5	4	2,4	4	2	8	1:1
Target C	5	3,8	2,6	4	2	8	1:3

Table 3.2: *Current Experimental Setup in amperes. For details, see figure: (3.1). N/A: not applicable*

The most important characteristic of the each test, is its cyclical nature at low frequency (1 program cycle each 300*msec*), in this sense the response of the system should be at low frequency. Consequently the voltage and power of the magnetron source shows a cyclical behavior. In the following group of graphics we can see this effect. Figures (3.5), (3.6), (3.7).

Target A

In Graph (3.5) we can see two complete cycles of the oscillation, where the power wave was selected as a reference of stability of the system, because of that the power magnetron signal represent two intrinsic signals (voltage and power), $P = V \cdot I$, for the case of the Target A (3.5), in the graphic of the power we can see that on the range between $(225 - 315)$ DAQ (*program cycles*), occurs a big variation in the wave, at the same time the voltage is in suturation.This means that for this combination of the current we have a critical point in the sputtering process. In other words is necessary to avoid this kind of the point in order to obtain a good model of control over the plasma confinement.

Target B

After to analyze the profile erosion result for the target A, and considering to avoid the critical point previously described, we can to modify the currents setup for the next test (Target B). In this sense is fixed a limit current for the (I_{ext}) equal to 8 Amps.

In group of the graph (3.6), we can see a little variation in the power wave in contrast with the variation previously observed in the graph (3.5), in fact it is avoided, but this condition can be produce a limit for the plasma on the center of the target. After compare the results obtained for the target A and B we can see a similar profile erosion pattern in both cases , but a reduction on percent of the material sputtered. This fact can be interpretated as a reduction of the area on the target available for to sputtering. In the next test will be modify the relative time between each half cycle. In order to maintain more time the plasma on the center region of the target.

Target C

In the following group of graphs (3.7), we can see the results obtained for the currents setup (target C). In the graph (3.7), we can see new forms of the instability in the power wave, which can be interpretated as a effect introduced by the velocity of change of the currents values in the coils, The results obtained for this experiment shows an increase of the percent of the material sputtered in contrast to the first tests.

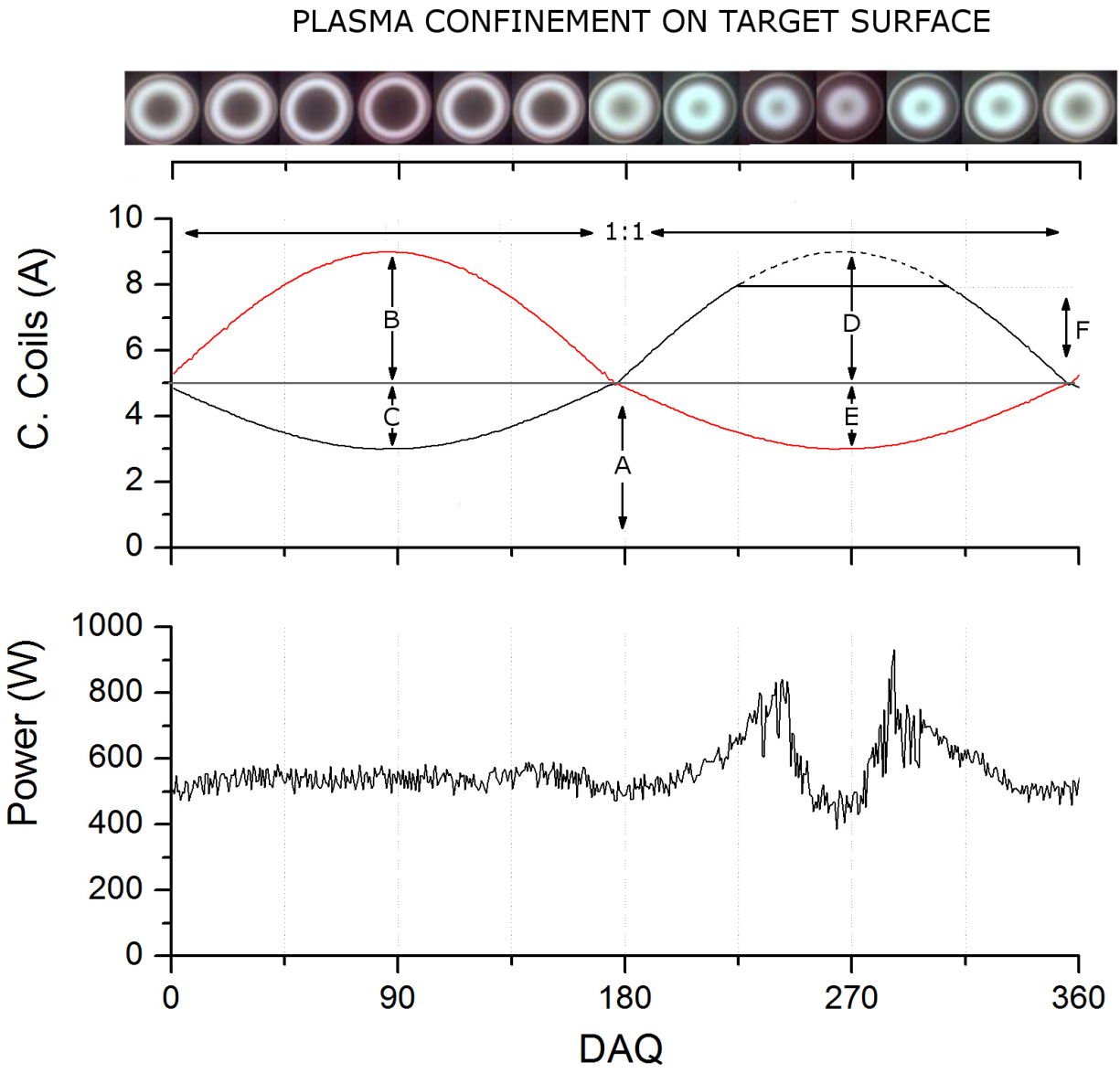

Figure 3.1: *Wave Currents setup and power magnetron source.* ***Legend:*** *A.-Offset. B.-Maximum peak I_{int} current. C.-Minimum peak I_{ext} current. D.-Maximum peak I_{ext} current. E.-Minimum peak I_{int} current. F.-Maximum out-current, I_{ext}. 1:1 .- Scale (Relative time between each half cycle.)*

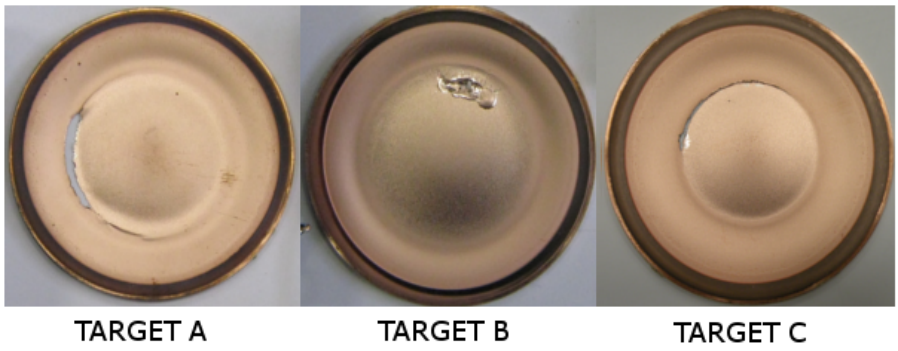

Figure 3.2: *Target erosion A-B-C*

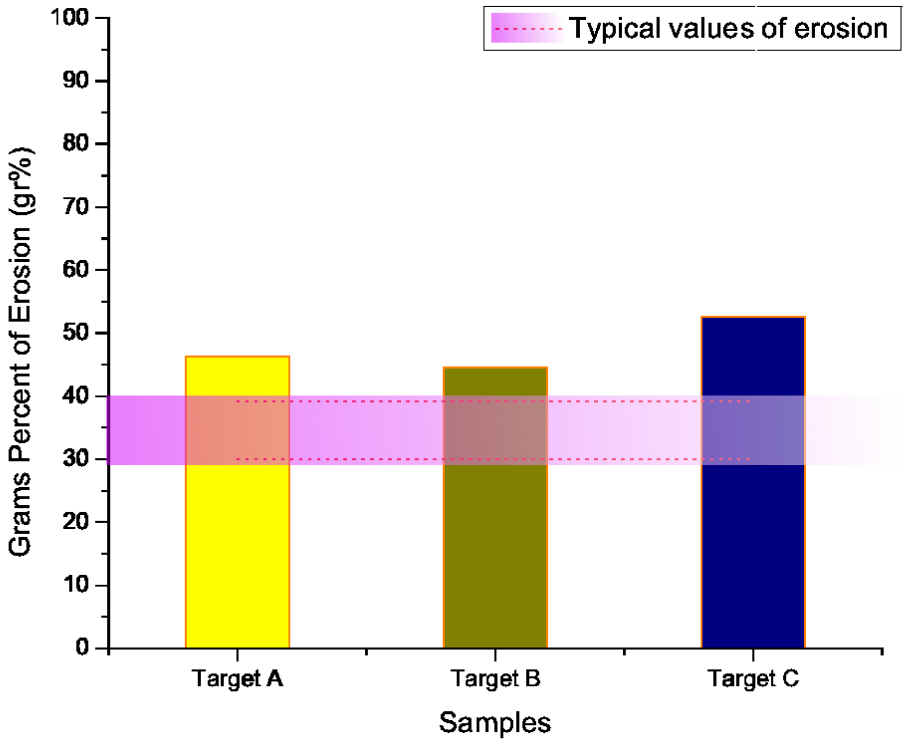

Figure 3.3: *Percent of target erosion A-B-C*

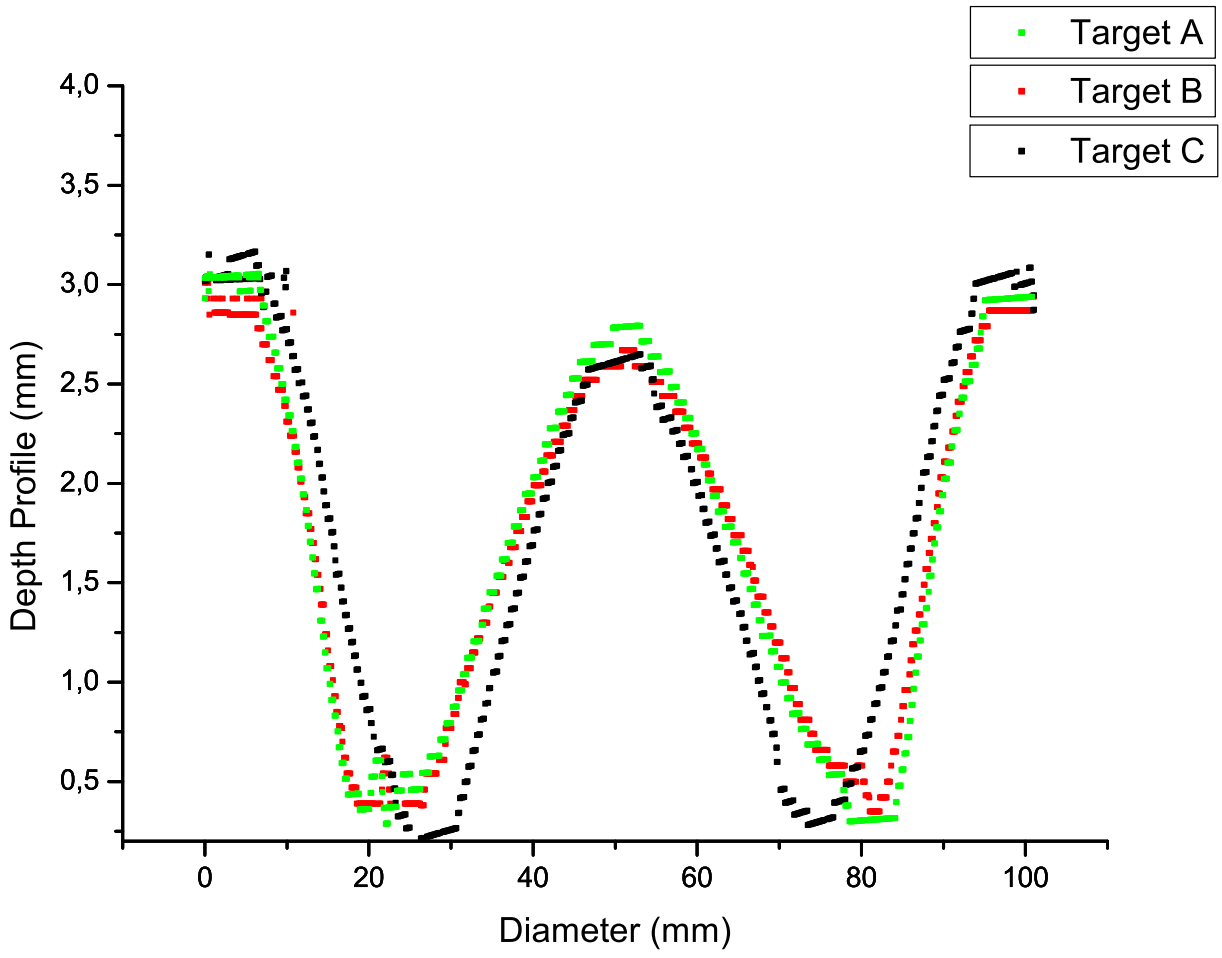

Figure 3.4: *Targets profile A-B-C*

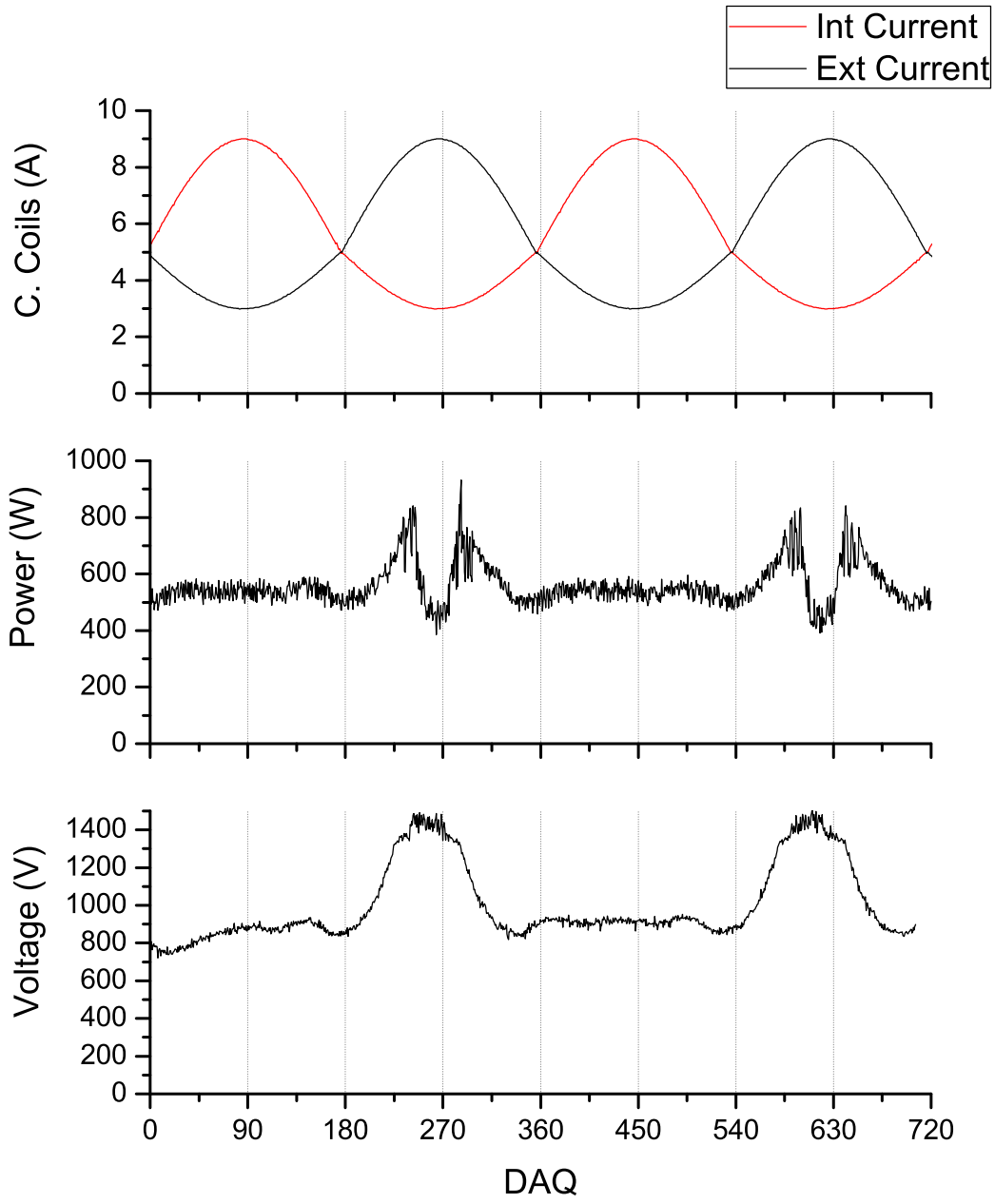

Figure 3.5: *Results target A: In the group of the graphs we can see the current waves setup (control), power and voltage waves magnetron (acquisition),obtained in the test: Target A.*

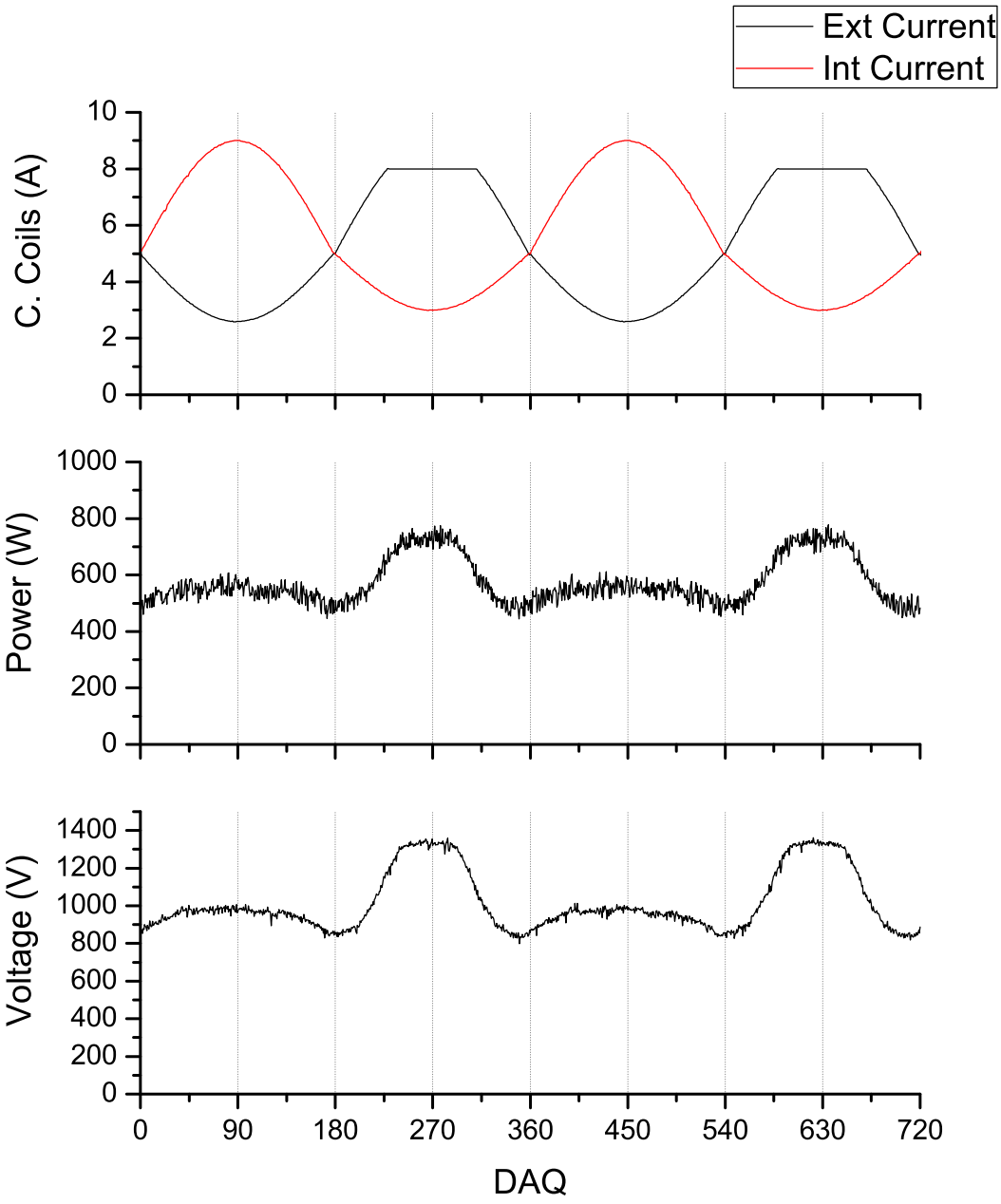

Figure 3.6: *Results target B: In the group of the graphs we can see the current waves setup (control), power and voltage waves magnetron (acquisition),obtained in the test: Target B.*

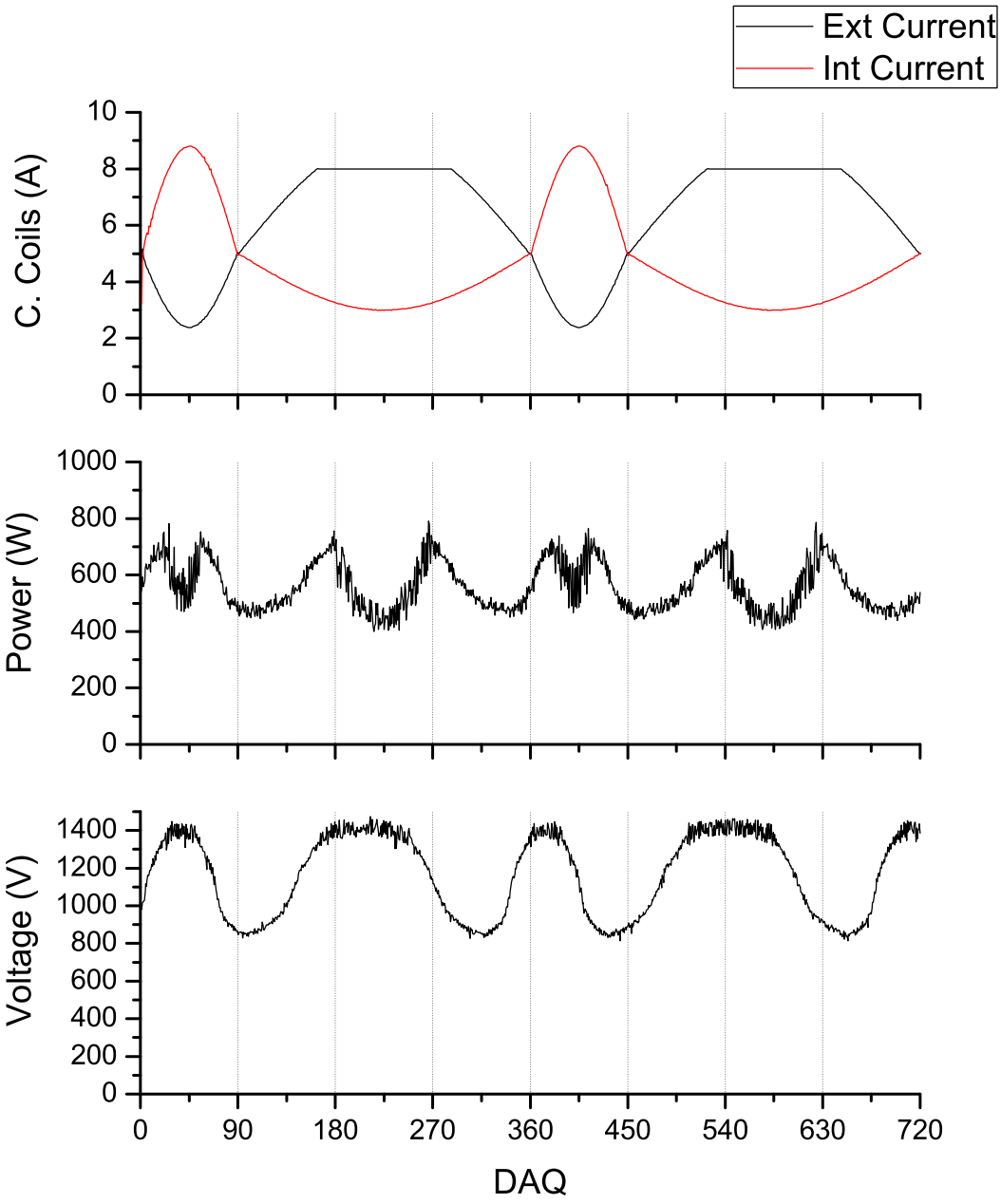

Figure 3.7: *Results target C: In the group of the graphs we can see the current waves setup (control), power and voltage waves magnetron (acquisition),obtained in the test: Target C.*

Chapter 4

Conclusions

Taking into account the theory studied, and therefore understanding how the variations of current affect the plasma confinement, an experimental system was created and designed in order to make several tests on the 4 sputtering source. In addition, it was created an experimental work plan built on a model of an open-loop control system, without the benefit of feedback, where the system is controlled directly, and only, by an input signal. Thanks to preliminary tests, the best parameter has been identified to control the erosion of the target. That parameter represents the basis of the program developed to control the system.

To obtain an efficient system was determined the minimum levels of the currents combination that permit to keep the plasma switched on.Sequential manual tests have successfully demonstrated the range of the current acceptable to confine the plasma over different regions of the target surface, calculated by the equations 2.1 and 2.2.As a consequence, these equations have been used as algorithm inside the program.

Thanks to the implementation of this algorithm to the system through the control program many tests have been done, but only three of them have given considerable results and so have been reported. The direct observation of the plasma on the target surface, the results of the erosion profile, and the quantity of sputtered material have been the basic criteria to justify the modification of the current setup for each different test.

The most important characteristic of each test was its cyclical natural behavior. This means that

it is possible to foresee a system reply based on the magnetron power. The main advantages of the system control program that has been implemented are revealed through the results obtained in this preliminary test.

This work centers its conclusions in the following opened arguments:

- The magnetron power represents a sign of stability of the magnetron sputtering
- The magnetron power represents a good promise as a signal feedback to control, automatically, to obtain the best erosion of the target.
- The speed of change of magnetic confinement could be a source of the non stability in the cyclic behavior of the power profile .
- To obtain the best erosion of the target in this system it is necessary to consider the optimization of the magnetic confinement and consider a possible physical modification of the magnetron source.

Further works:

Starting from these results, we want, in future, to optimize the target erosion changing the current of the magnetic confinement of the two coils, through the control of the magnetron power, in order to obtain an efficiency close to 80% of the erosion.

Bibliography

[1] John.L.Vossen:Werner.Kern.
Thin film processes II.
Book, Vac-Tec Systems, Inc. Boulder, Colorado.

[2] Chris.M.Horwitz.
Hollow cathode etching and deposition, Chapter.12.
Handbook of Plasma Processing Technology.

[3] R.V.Stuart.
Vacuum technology, thin films, and sputtering an introduction.
Book, Koral Labs, Inc. Minneapolis, Minnesota. 1983.

[4] R.V.Stuart.
CAD for Electromagnetic Devices.
Paper, Koral Labs, Inc. Minneapolis, Minnesota. 1983.

[5] QIU.Qingquan.:LI.Quingfu.:SU.Jingjing.:JIAO.Yu.: FINLEY.Jim.
Simulation to predict target erosion of planar DC magnetron.
Plasma Science and Technology, Vol.10,Nro.5,Oct.2008.

[6] Chae-Hwa.SHON.:Uk-sung.KIM.:Deok-Woo.HAN.:Youl-Moon SUNG.
Enhancement of usage of cathode Materials.
J.Plasma Fusion Res. SERIES, Vol.8.2009.

[7] N.N.Losad.:B.D.Jackson.:F.Ferro.:J.R.Gao.:S.N.Polyakov.:P.N.Dmitriev.:T.M.Klapwijk.
Source optimization for magnetron sputter-deposition of NbTiN tuning elements for SIS THz detectors.
Supercond.Sci.Technol.12(1999)736-740.

[8] QIU.Qingquan.:LI.Quingfu.:SU.Jingjing.:JIAO.Yu.: FINLEY.Jim.
Magnetic field improvement in end region of rectangular planar DC magnetron based on particle simulation.
Plasma Science and Technology, Vol.10,No.6, Dec.2008.

[9] T.Kubart.:R.Nov k.:J.Valter.
Modeling of magnetron sputtering process.
Czechoslovak Journal of physics, Vol.54 (2004), Suppl. C.

[10] M.Lavarone:A.Andreone.:P.Orgiani.:G.Pica:M.Salluzo:R.Vaglio:LL.Kulyk:V.Palmieri.
A simple and reliable system for in situ deposition of large-area double-side, superconducting films.
Supercond.Sci.Technol., Vol.13 (2000), Pages 1441-1446.

[11] V.Palmieri.:G.Keppel.:I.Kulyk.:D.Tonini.
Engineering of magnetron sputtering sources for thin film deposition
Instituto nazionale di Fisica Nucleare- Laboratori Nazionali di Legnaro, Legnaro (Padua)

[12] Y.Kusumoto.:K.Iwata.
Numerical study of the characteristics of erosion in magnetron sputtering.
Ulvac Technical Journal (English) N63E 2006.

[13] Anila Gottschling
Feasibility study of sputtered radiofrequency quadrupole
Thesis Book,Instituto Nazionali di Fisica Nucleare. Padova, May 2002.

[14] Windows.B.:Savvides.N 1986 J. Vac. Sci. Technol, A 4 196

[15] ftp://ftp.testequity.com/pdf/603x.pdf

[16] Windows.B.:Harding G.L 1986 J. Vac. Sci. Technol, A 4 196

[17] $http://www.io.com/\ wazmo/papers/seven_steps.html$

[18] http://www.sls.psi.ch/controls/hardware/pdf/pfeiffer-TPG-262.pdf